Steel and Composite Structures, *Vol. 18, No. 6 (2015) 1479-1492*
DOI: http://dx.doi.org/10.12989/scs.2015.18.6.1479

Stress distribution on the real corrosion surface of the orthotropic steel bridge deck

Shigenobu Kainuma [1a], Young-Soo Jeong [1b] and Jin-Hee Ahn [*2]

[1] *Department of Civil Engineering, Kyushu University, 819-0395, Fukuoka, Japan*
[2] *Department of Civil Engineering, Gyeongnam National University of Science and Technology, 660-758, Jinju, Gyeongnam, Korea*

(*Received March 16, 2013, Revised May 19, 2014, Accepted December 08, 2014*)

Abstract. This study evaluated the localized stress condition of the real corroded deck surface of an orthotropic steel bridge because severe corrosion damage on the deck surface and fatigue cracking were reported. Thus, a three-dimensional finite element (FE) analysis model was created based on measurements of the corroded orthotropic steel deck surface to examine the stress level dependence on the corrosion condition. Based on the FE analysis results, it could be confirmed that a high stress concentration and irregular stress distribution can develop on the deck surface. The stress level was also increased by approximately 1.3-1.5 times as a result of the irregular corroded surface. It was concluded that this stress concentration could increase the possibility of fatigue cracking in the deck surface because of the surface roughness of the orthotropic steel bridge deck.

Keywords: real corroded surface; orthotropic steel deck; stress level; principal stress; FE analysis

1. Introduction

An orthotropic steel bridge deck, which consists of a longitudinal deck, ribs, and floor beams, directly resists loads and transmits them to the main structure. This structure has been used in various steel bridges because it is lightweight compared to traditional reinforced concrete decks. However, diverse fatigue cracks have also been reported on the deck plate–rib and rib–floor beam welds as a result of their relatively slender geometries (Pfeil *et al*. 2005, Battista *et al*. 2008). Corrosion problems are not usually considered for the deck surface because of the use of a waterproofing layer consisting of an anti-corrosion coating or paint. However, severe corrosion damage on the deck surface of an orthotropic steel bridge deck and fatigue cracking have been reported, as shown in Fig. 1(a), even though an anti-corrosion coating was applied to the deck surface (Sakiya *et al*. 2007). Thus, to examine this corrosion problem, the structural responses of an orthotropic steel deck with a corroded deck surface were analytically evaluated using a three-dimensional finite element (FE) analysis model (Frýba and Urushadze 2011, Kainuma *et al*.

∗Corresponding author, Assistant Professor, Ph.D., E-mail: jhahn@gntech.ac.kr
[a] Ph.D., E-mail: kai@doc.kyushu-u.ac.jp
[b] Ph.D., E-mail: jeong@doc.kyushu-u.ac.jp

 ISSN: 1229-9367 (Print), 1598-6233 (Online)

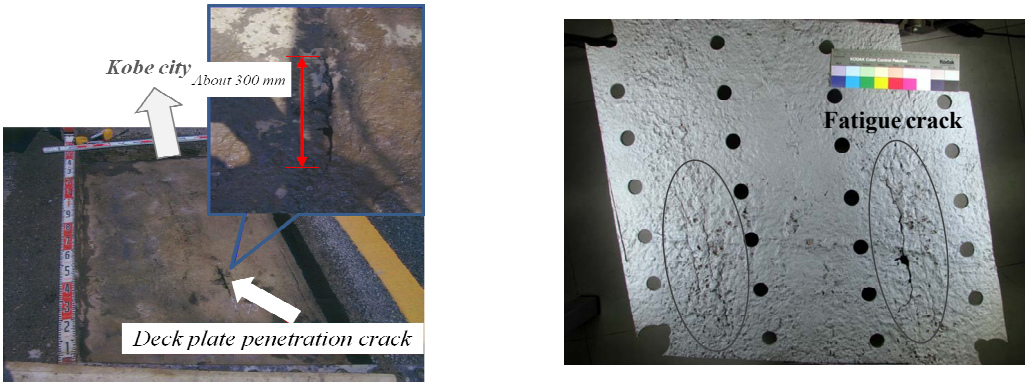

(a) Fatigue crack on the corroded deck surface (b) Real corroded deck surfaces image

Fig. 1 Fatigue crack on the corroded deck surface of the orthotropic steel bridge deck (Sakiya *et al*. 2007)

1996). In the case of the previous research, two corroded surface models were used to investigate the stress level on the corroded surface, including a mean corroded surface model and corroded surface model, which considered how the deck thickness changed depending on the corrosion damage. The material proprieties of asphalt were also changed in response to seasonal temperature changes to determine the effects of the material proprieties of asphalt on the structural behaviors of an orthotropic steel deck (Jeong *et al*. 2013). The possibility of fatigue cracking was also examined in relation to the corroded surface level and condition. However, artificially corroded surfaces were used, which were generated based on a spatial statistical simulation method using a variogram from the spatial information of a corroded surface, instead of using a real corroded surface (Kainuma *et al*. 2012). Thus, those results could not reflect a real corroded surface condition. Therefore, in this study, areal corroded orthotropic steel deck was considered, and the corrosion conditions were examined in terms of the mean corrosion depth and maximum corrosion depth using laser scanning. Then, an FE analysis was carried out to examine the localized stress condition of the corroded deck surface using a three-dimensional FE analysis model to simulate the measured corroded deck surface.

2. Evaluation of the corroded deck suface in the real orthotropic deck

Fig. 1(b) shows the corroded deck surface of an orthotropic steel bridge deck after removing the surface rust. As shown in Fig. 1(b), the severe roughness of the deck surface could be confirmed to be as much as the 4-7 mm on the corroded surface. It was divided into six corroded surface models to determine the corrosion conditions. Fig. 2 presents corroded depth surface images from laser scanning at a distance of 0.4 mm. The weight loss of the test specimen was measured using an electronic balance. The surface morphology of the test specimen was characterized using laser scanning (spot diameter 30 μm; resolution 0.05 μm). With reference to the preliminary surface roughness monitoring results using the laser scanning, the measurement distance was 0.4 mm. From the surface roughness profile evaluated using the laser measurements with reference to the intact surface level, the mean corrosion depth was calculated by determining the measured weight loss distributed proportionally to the measured surface roughness. Fig. 3 shows a histogram of

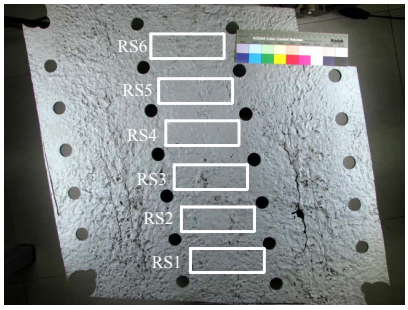

(a) Specimens location on orthotropic steel deck

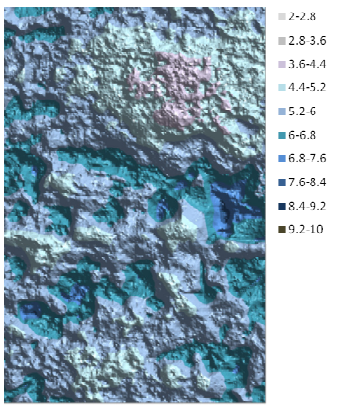

(i) Corroded surface RS1

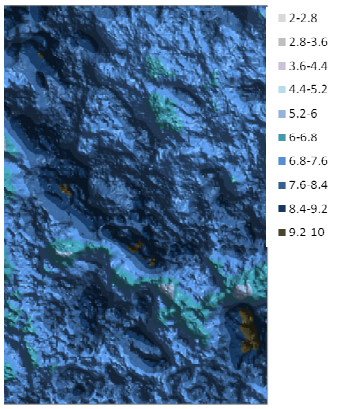

(ii) Corroded surface RS2

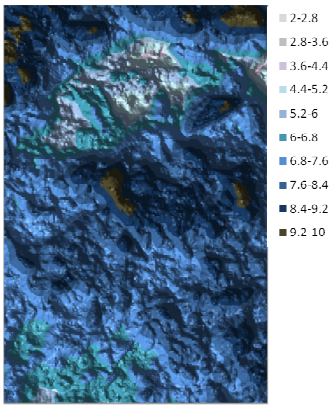

(iii) Corroded surface RS3

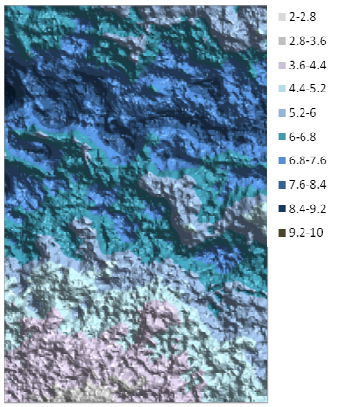

(iv) Corroded surface RS4

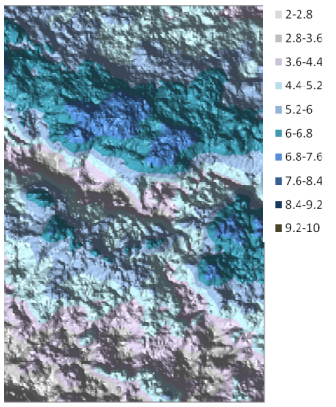

(v) Corroded surface RS5

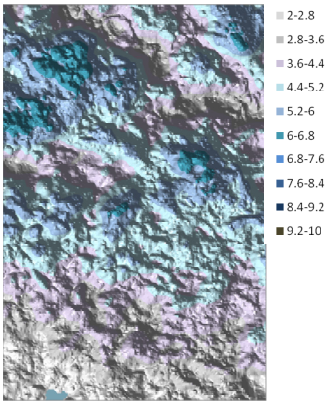

(vi) Corroded surface RS6

(b) Corroded surface image on specimens

Fig. 2 Real corroded deck surfaces image of the cut orthotropic steel deck

each real corroded surface model. As shown in Figs. 2-3, the corrosion level and distribution of the deck surface changed sharply and irregularly depending on the deck surface area of the orthotropic steel bridge deck, similar to their standard distribution. The mean and maximum corrosion depths measured by laser scanning are listed in Table 1.

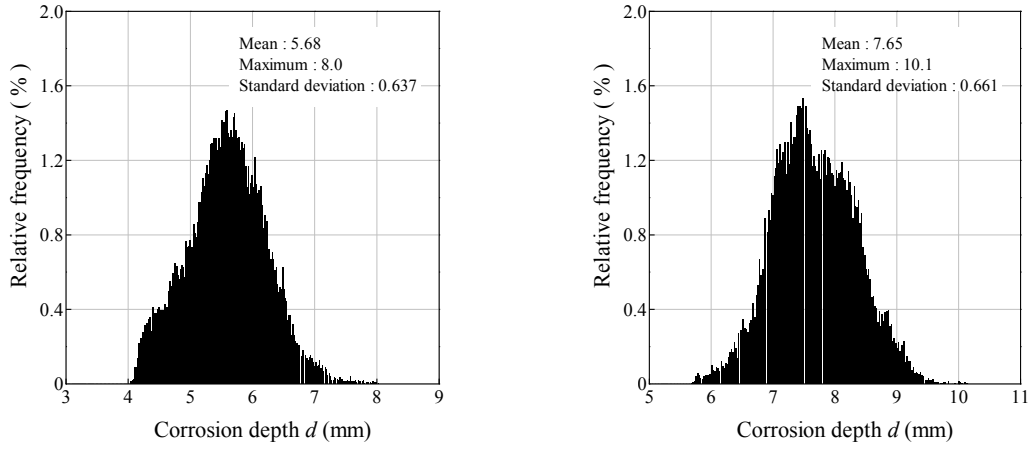

(a) Corroded surface RS1

(b) Corroded surface RS2

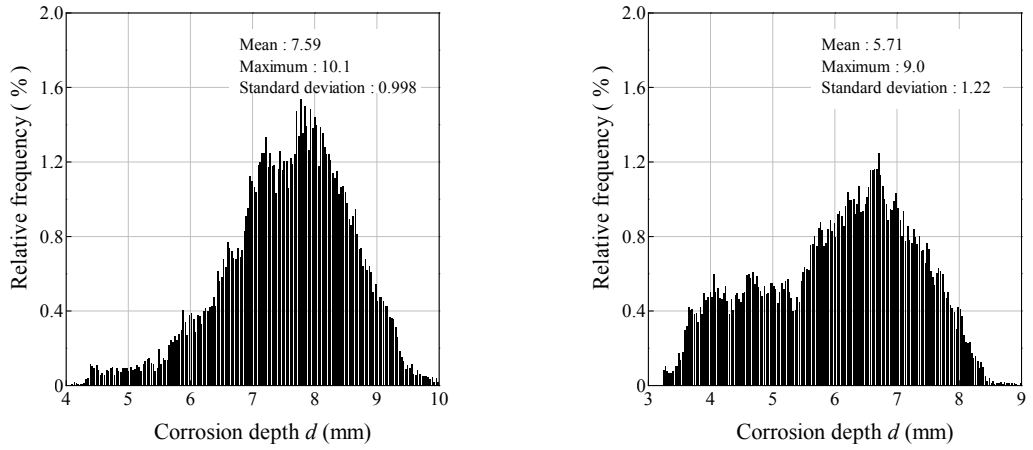

(c) Corroded surface RS3

(d) Corroded surface RS4

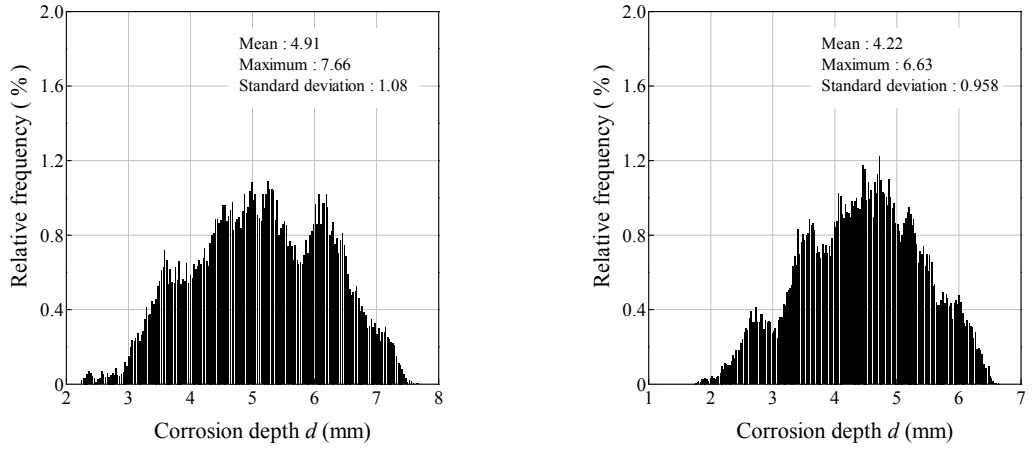

(e) Corroded surface RS5

(f) Corroded surface RS6

Fig. 3 Histogram of real corroded deck model

Table 1 Surface data of the corroded deck surface (unit: mm)

Corroded surface	Mean corroded depth	Maximum corroded depth	Minimum corroded depth	Standard distribution
RS1	5.68	8.0	4.04	0.64
RS2	7.65	10.1	5.68	0.66
RS3	7.59	10.1	4.08	1.00
RS4	5.71	9.0	3.21	1.22
RS5	4.91	7.66	2.23	1.08
RS6	4.22	6.63	1.75	0.96
Avg.	5.96	8.59	3.50	0.93

3. FE analysis model of corroded deck surface in the orthotropic deck

An orthotropic steel bridge deck stiffened with closed U-ribs was used to evaluate the stress distribution on a corroded deck surface. It had a height of 560 mm, width of 3,200 mm, floor beam span length of 2,512 mm, and 80 mm of asphalt pavement, as shown in Fig. 4. The thicknesses of the deck and closed U-ribs were 12 mm and 6 mm, respectively. A three-dimensional FE analysis model was created using the MARC mentat 2010 application. To evaluate the behaviors of the orthotropic steel deck with a corroded deck surface, the structural members (the deck plate, ribs, and asphalt pavement) of the orthotropic steel deck were modeled using eight-node solid elements (hex8). The localized stress condition of the corroded deck surface was examined to use a real corroded surface model, wherein the deck thickness was equivalently decreased based on the corrosion level of the real corroded surface model. This model was applied to the deck surface at the U-rib-deck plate welding connections, where the maximum tensile stress occurred by vehicle

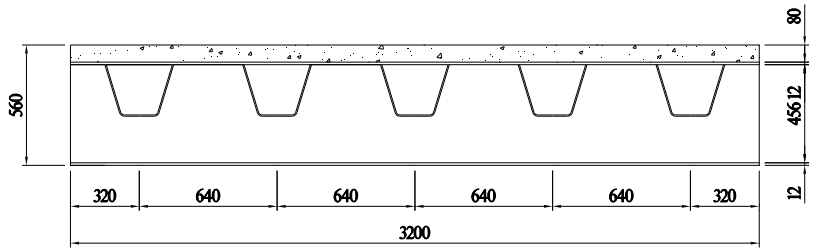

(a) Front view

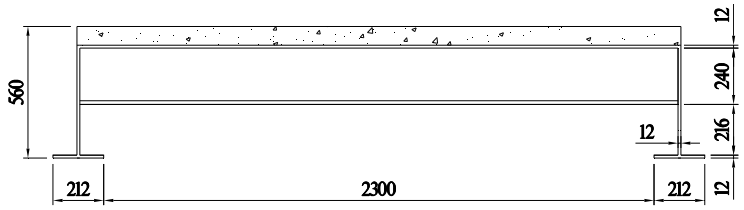

(b) Side view

Fig. 4 Dimension of the orthotropic steel deck steel box bridge with U rib (unit: mm)

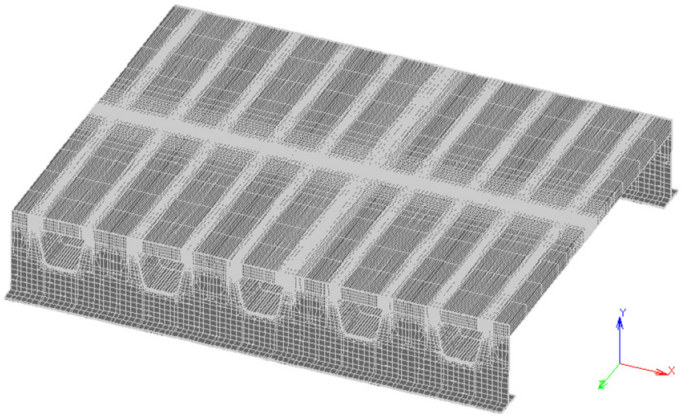

(a) FE analysis model

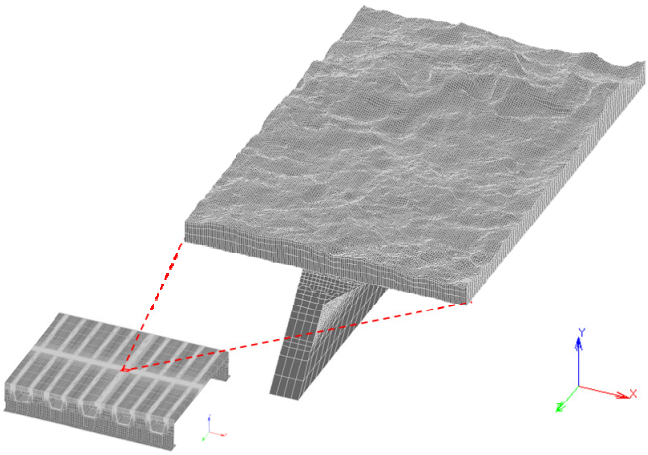

(b) Mesh of corroded surface model in FE analysis

Fig. 5 FE analysis model of the orthotropic steel bridge deck

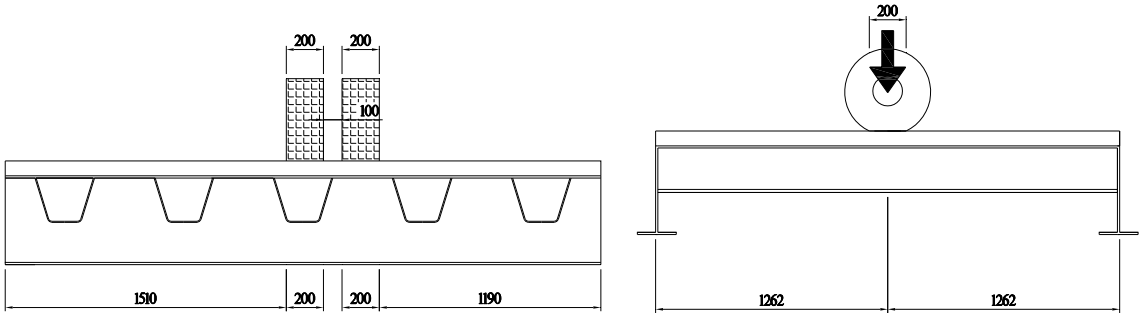

(a) Front view (b) Side view

Fig. 6 Loading conditions of the orthotropic steel deck (unit : mm)

loading. In total, the structural responses of six models with corrosion depths of 5.68 mm, 7.65 mm, 7.59 mm, 5.71 mm, 4.91 mm, and 4.22 mm were compared and evaluated. The FE analysis model and mesh of the corroded surface model of the orthotropic steel bridge deck are shown in Fig. 5. Fig. 6 shows a truck tire load of 100 kN applied to the FE analysis model to develop the maximum negative moment at the deck surface at the U-rib-deck plate welding connection. The steel grade of the orthotropic deck model was assumed to be SM490, which has yield strength of 320 MPa. An elastic modulus of 206,000 MPa and Poisson's ratio of 0.35 were applied as the steel material properties, and a value of 500 MPa was used as the elastic modulus of the asphalt pavement during the summer season (Cheng *et al*. 2004).

4. Stress concentration of corroded surface in orthotropic steel deck

In the previous study, the deformations and stress distributions calculated using a mean corroded surface model were evaluated and compared according to the corrosion level (mean corrosion depth) and seasonal stiffness variation of the asphalt pavement to examine how the structural behaviors of an orthotropic steel deck depended on the corrosion level (flat surface model) (Jeong *et al*. 2013). The displacements of the orthotropic steel deck were shown to increase and shift slightly toward the U-rib depending on the corrosion level (flat surface model). Stress distribution was observed in a welding connection of the lower deck surface in terms of the stress concentration in the deck surface without using a corroded surface model; the stress distribution depended on the moment distribution of the deck plate, which resulted from a loading condition and high stress values (Jeong *et al*. 2013). Therefore, in this study, the deformations and stress distributions calculated from the mean corroded surface model were not compared in relation to the corrosion level, but the principal stress distributions of the corroded surfaces were examined to

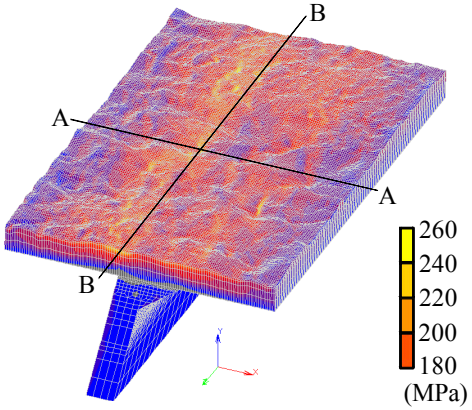

(i) Contour of principal stress

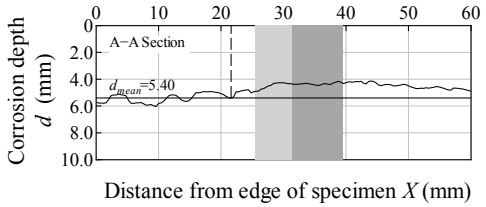

(ii) Corrosion depth distribution on A-A section

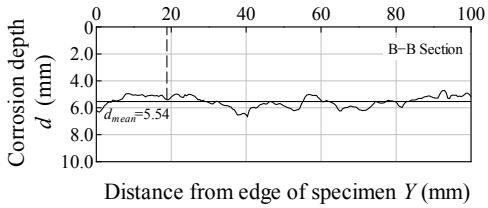

(iii) Corrosion depth distribution on B-B section

(a) Corroded surface RS1

Fig. 7 Maximum principal stress of corroded surface model

determine the possibility of fatigue cracking based on the localized stress concentration of the corroded deck surface.

4.1 Maximum principal stress distribution

To examine the local stress distributions on the corroded surfaces, their principal stress distributions were identified using the location of the maximum principal stress for each of the corroded surface models, because the local stress concentration developed by the uneven deck

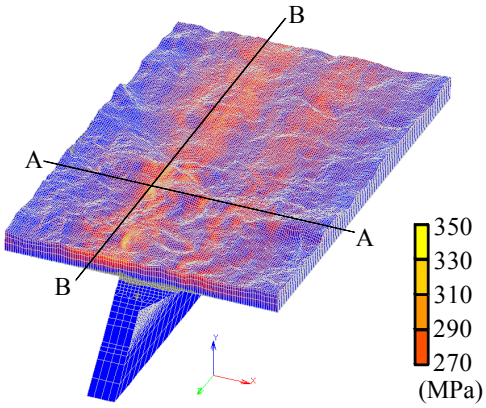

(i) Contour of principal stress

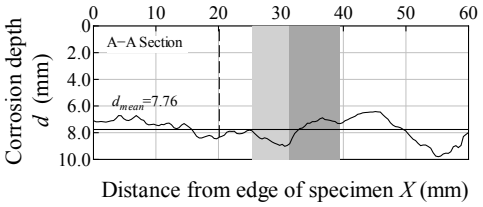

(ii) Corrosion depth distribution on A-A section

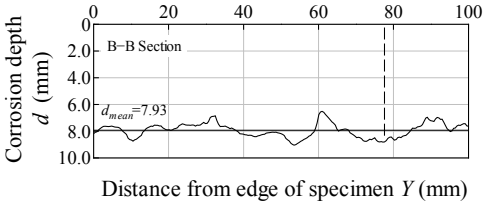

(iii) Corrosion depth distribution on B-B section

(b) Corroded surface RS2

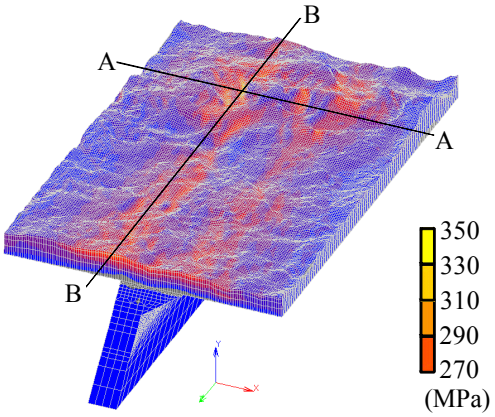

(i) Contour of principal stress

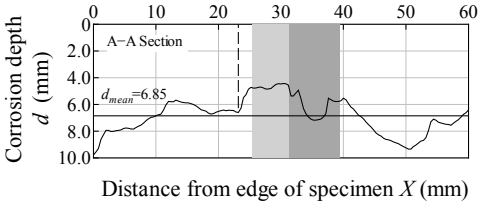

(ii) Corrosion depth distribution on A-A section

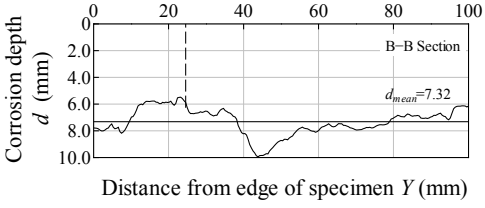

(iii) Corrosion depth distribution on B-B section

(c) Corroded surface RS3

Fig. 7 Continued

plate surface could cause fatigue cracking in the deck plate (Battista and Pfeil 2004, Connor and Fisher 2005, Wolchuk 1990, Yoshihiko *et al*. 2009, Choi *et al*. 2008). The maximum principal stress contours and maximum principle stress locations of the corroded orthotropic bridge deck surface are presented in Fig. 7. As shown in Fig. 7, the maximum principle stresses appeared around the U-rib and deck plate connection area, and these were slightly higher than that of the un-corroded deck plate by 2.39, 3.39, 3.18, 2.50, 2.27, and 2.12 times. This occurred because of the thickness decreases and irregular surfaces of the deck plate caused by corrosion. The principal stress distributions at the maximum principal stress sections were also compared in the longitudinal and transverse directions, as shown in Fig. 8. The principal stress distributions of the

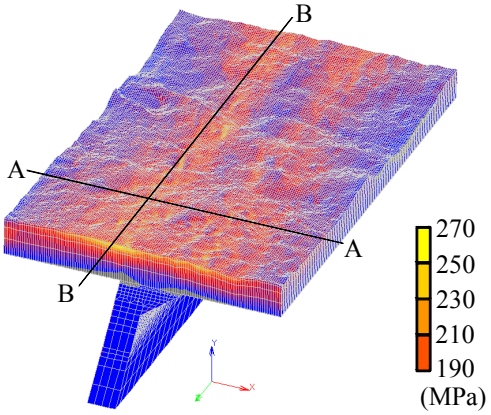

(i) Contour of principal stress

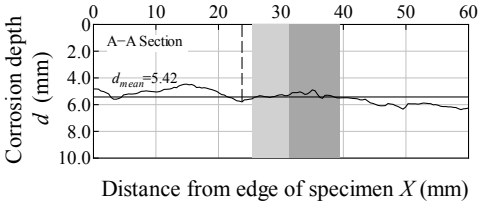

(ii) Corrosion depth distribution on A-A section

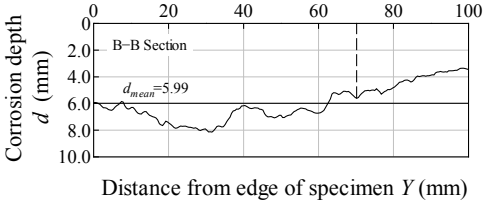

(iii) Corrosion depth distribution on B-B section

(d) Corroded surface RS4

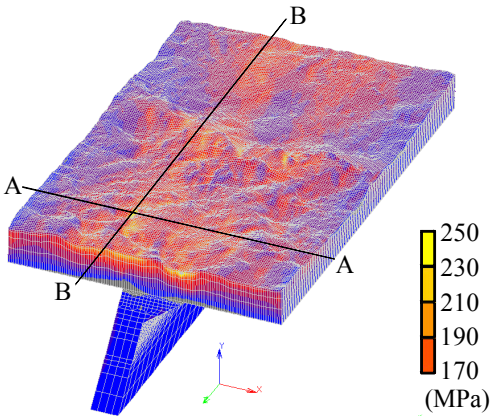

(i) Contour of principal stress

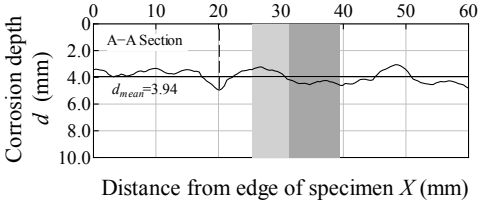

(ii) Corrosion depth distribution on A-A section

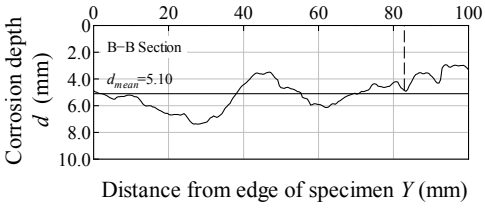

(iii) Corrosion depth distribution on B-B section

(e) Corroded surface RS5

Fig. 7 Continued

corroded surface model were shown to be irregular, according to the roughness of the uneven corroded deck surfaces shown in Figs. 7-8. The principal stress was shown to vary greatly according to the change in roughness.

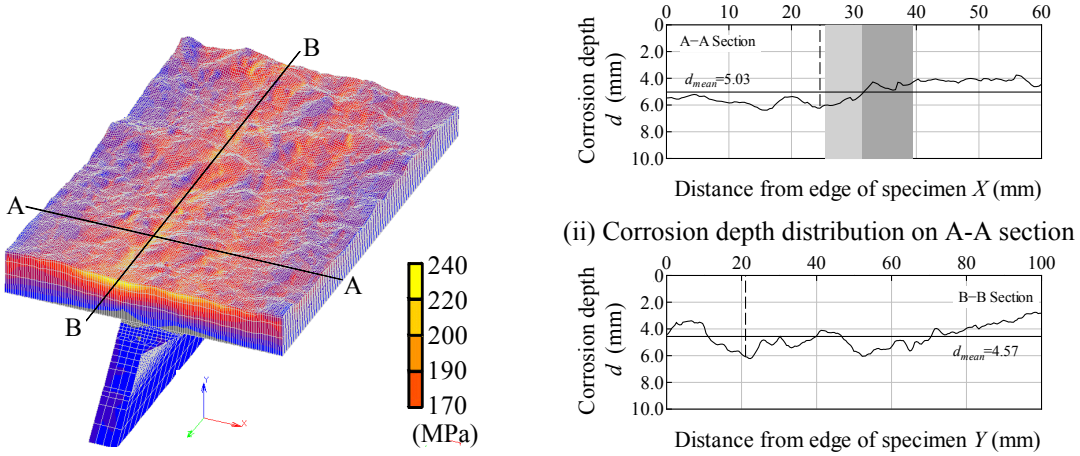

(i) Contour of principal stress

(ii) Corrosion depth distribution on A-A section

(iii) Corrosion depth distribution on B-B section

(f) Corroded surface RS6

Fig. 7 Continued

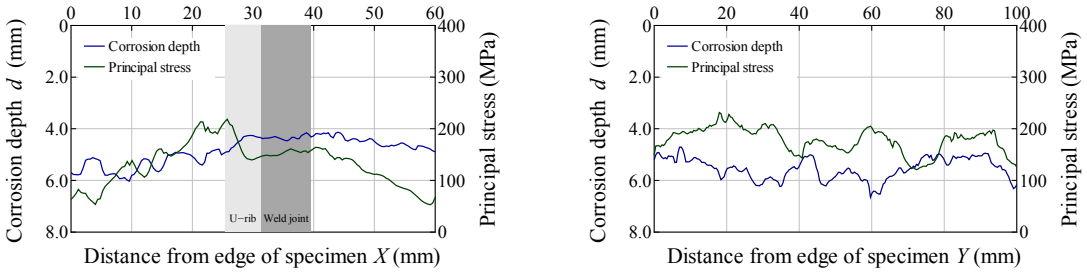

(a) Corroded surface RS1

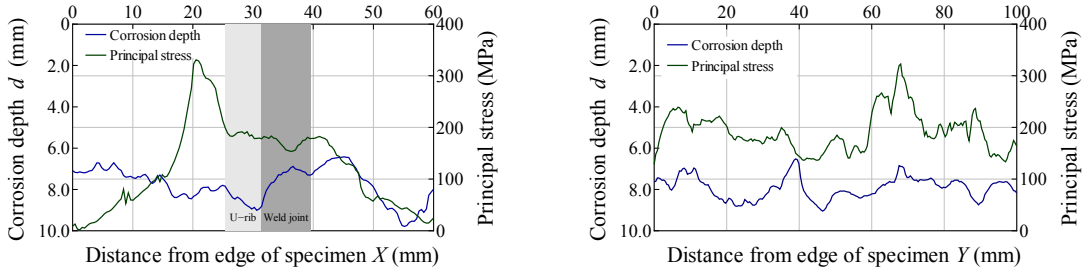

(b) Corroded surface RS2

Fig. 8 Principal stress distributions of the corroded surface model

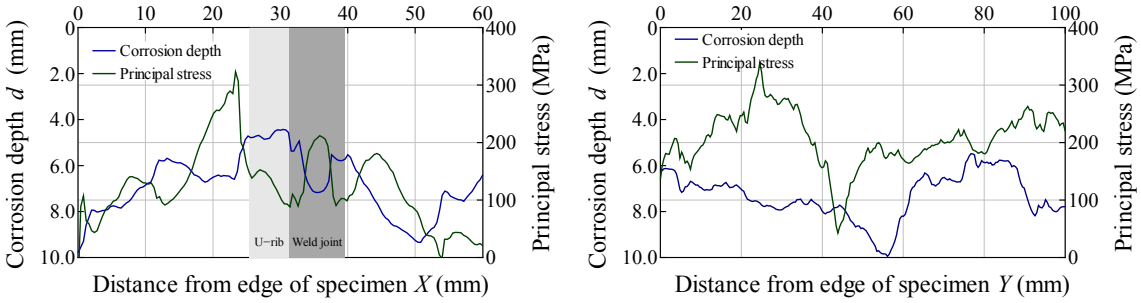

(c) Corroded surface RS3

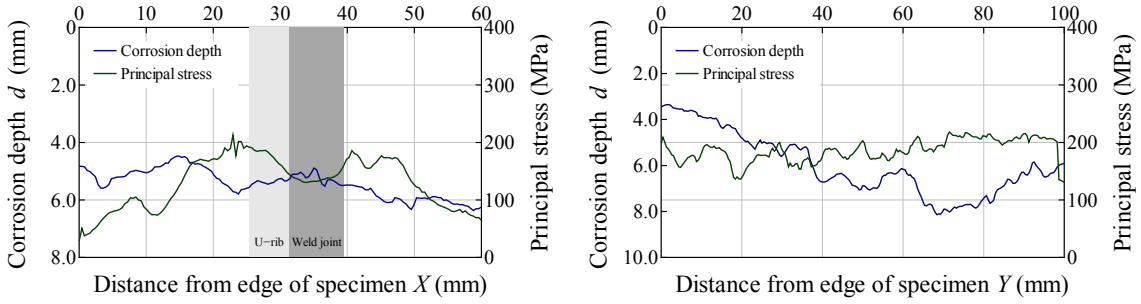

(d) Corroded surface RS4

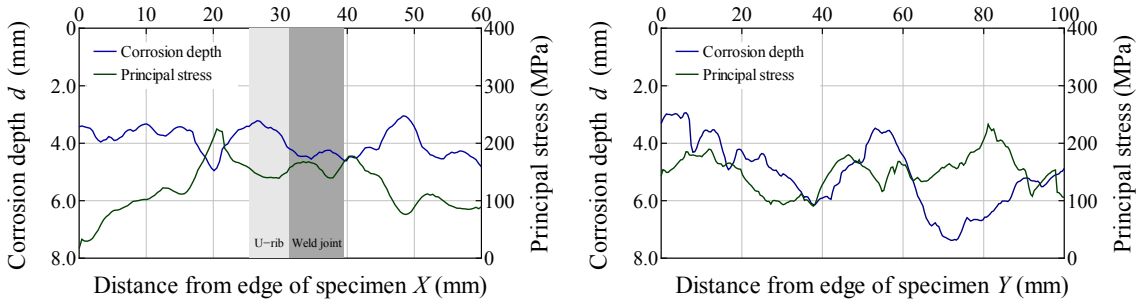

(e) Corroded surface RS5

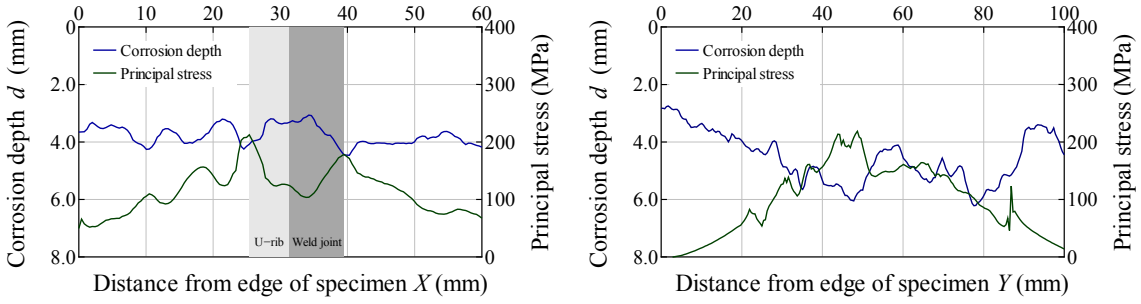

(f) Corroded surface RS6

Fig. 8 Continued

4.2 Fatigue strength evaluation of the corroded deck surface

To evaluate the change in the stress level according to the corrosion damage on the orthotropic bridge deck, the maximum principal stress was compared with FE analysis results without the irregular corroded surface (flat surface model) depending on the mean corroded thickness of the real corroded deck model (Jeong *et al*. 2013). Fig. 9 shows the maximum principle stress and mean corroded thickness relationships. For the FE analysis results without the irregular corroded surface (flat surface model), the maximum principle stress increased in proportion to the corrosion level, with a stress change of 16.8 per unit of corroded depth (Jeong *et al*. 2013). In the case of the real corroded surface model, the maximum principle stress also increased in proportion to the corrosion level, similar to the flat surface model and the gradient was found to be 28.0. It could be confirmed that the stress change of the real corroded surface model was higher than that of the flat surface model, as shown in the regression curves of Fig. 9. For each corroded surface model, the principal stress ratio was calculated using the decrease in the deck thickness and the irregular corroded surface of the real corroded deck model using the regression curve of the flat surface model in Fig. 9. The results are summarized in Table 2. The corroded thickness was found to increase by approximately 1.6-2.2 times, and the stress level also increased by approximately 1.3-1.5 times because of the increase in the principal stresses by the corroded roughness. Therefore, it was found that the irregular corroded surface could cause increases in the stress and stress concentration as a result of the surface form.

To simply examine the possibility of fatigue cracking on the corroded deck surface, the stress levels of the corroded surface models were compared with the specifications in IIW and AASHTO, as shown in Fig. 10. The structural performance of a corroded steel structure may decrease as a result of the loss of sectional properties by corrosion damage. It can be evaluated by considering the decreased sectional properties, although this approach is not an established one. However, it is more difficult to estimate or predict the occurrence of corrosion fatigue failure in structural members because the corrosion phenomena differ with the corrosion environment. The deck plate of the orthotropic bridge deck could also be given an A grade because the fatigue category could be given an A grade based on the fatigue strength of a flat plate. The stress levels of the six corroded surface models exceeded the fatigue limit of stress category A because of the stress

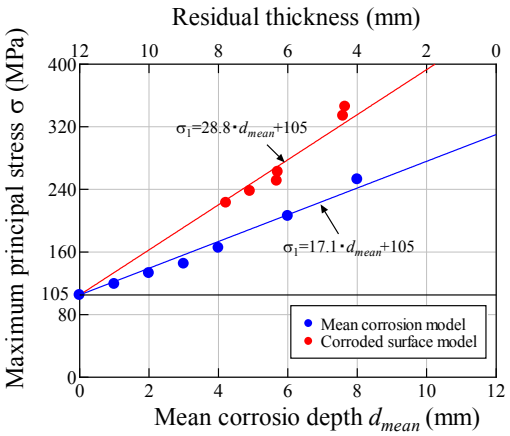

Fig. 9 Maximum principal stress and mean corrosion depth relationships

Table 2 Surface data of the corroded deck surface (unit: mm)

Corroded surface	Mean corroded depth	Maximum principal stress	Stress ratio by the deck thickness	Stress ratio by the corroded surface
RS1	4.22	223	1.65	1.29
RS2	4.91	238	1.75	1.29
RS3	5.71	263	1.88	1.33
RS4	7.59	334	2.16	1.47
RS5	7.65	346	2.17	1.52
RS6	5.68	251	1.87	1.28
Avg.	5.96	276	1.91	1.36

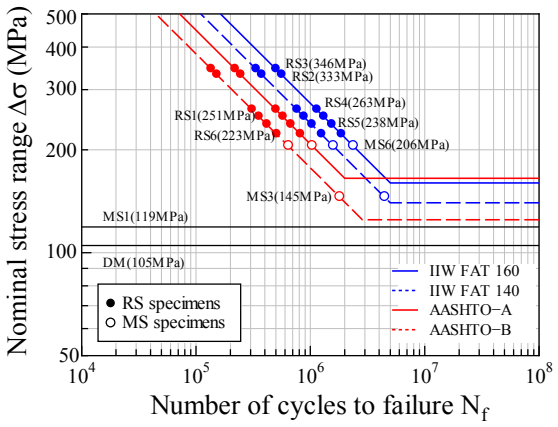

Fig. 10 S-N curves comparisons

concentration generated by the surface roughness. Therefore, fatigue cracks could occur on the deck surface from the stress concentration developed by the corroded surface roughness of the orthotropic steel bridge deck.

5. Conclusions

In this study, the localized stress condition of a corroded deck surface was examined using a three-dimensional FE analysis model that was based on surface measurements of a real corroded orthotropic steel deck. To evaluate the corroded surface condition, the corrosion conditions were measured using laser scanning. The maximum principal stresses were examined using FE analyses, and the possibility of fatigue cracking was examined based on the stress concentration of the irregular corroded surface. From the FE analysis results, it could be confirmed that a corroded surface can develop a high stress concentration and irregular stress distribution on the deck surface from the surface roughness generated by corrosion. Based on this stress concentration on the corroded surface, it was found that fatigue cracking on the deck surface was caused by severe corrosion damage to the deck surface of an orthotropic steel bridge deck.

References

American Association of State Highway and Transportation Officials (AASHTO) (1998), LRFD Bridge Design Specifications; (2nd Ed.), Washington D.C., USA.

Battista, R.C. and Pfeil, M.S. (2004), "Strengthening fatigue-cracked steel bridge decks", *J. Bridge Eng*., **157**(2), 93-102.

Battista, R.C., Pfeil, M.S. and Carvalho, E.M.L. (2008), "Fatigue life estimates for a slender orthotropic steel deck", *J. Construct. Steel Res*., **64**(1), 134-143.

Cheng, X., Murakoshi, J., Nishikawa, K. and Ohashi, H. (2004), "Local stresses and fatigue durability of asphalt paved orthotropic steel decks", *Proceedings of 2004 Orthotropic Bridge Conference*, Sacramento, CA, USA, August.

Choi, S.M., Tateishi, K., Kim, I.T., Seo, W.C. and Lee, D.U. (2008), "Fatigue strength improvement of U-type trough rib at field Welded Joint in steel bridge deck", *Int. J. Steel Struct*., **8**(3), 215-223.

Connor, R.J. and Fisher, J.W. (2005), "Field testing of orthotropic bridge decks", *Int. J. Steel Struct*., **5**(3), 225-231.

Frýba, L. and Urushadze, Sh. (2011), "Improvement of fatigue properties of orthotropic decks", *Eng. Struct*., **33**(4), 1166-1169.

International Institute of Welding (IIW) (2008), Recommendations for Fatigue Design of Welded Joints and components; XIII-2151r4-07/XV-1254r4-07, New York, NY, USA.

Jeong, Y.S., Kainuma, S. and Ahn, J.H. (2013), "Structural response of orthotropic bridge deck depending on the corroded deck surface", *Construct. Build. Mater*., **43**, 87-97.

Kainuma, S., Yamada, K., Johsen, Y., Iwasaki, M. and Nishikawa, T. (1996), "Test and analysis of Influence of cracked ribs on orthotropic steel deck", *J. Struct. Eng*., **42A**, 927-936. [In Japanese]

Kainuma, S., Jeong, Y.S., Utsunomiya, K. and Ahn, J.H. (2012), "Numerical simulations for time-dependent corrosion surfaces of unpainted carbon steel plates in atmospheric corrosive environments using spatial statistical techniques", *Corrosion Eng*., **61**(7), 203-212.

Pfeil, M.S., Battista, R.C. and Mergulhão, A.J.R. (2005), "Stress concentration in steel bridge orthotropic decks", *J. Construct. Steel Res*., **61**(8), 1172-1184.

Sakiya, K., Sugiyama, Y. and Yoshiyuki, T. (2007), "Crack penetration of orthotropic steel bridge deck by corrosion in Nishinomiya Osaka line", *Proceedings of the 42nd Hanshin Expressway Technical Research Conference*, Osaka, Japan, May. [In Japanese]

Wolchuk, R. (1990), "Lessons from weld cracks in orthotropicdecks on three European bridges", *J. Struct. Eng*., **116**(1), 75-84.

Yoshihiko, T., Minoru, K., Takashi N. and Kimihisa, U. (2009), "Fatigue failure assessment of actual-working load and run location on orthotropic steel deck applied in BWIM", *J. Struct. Eng*., **55A**, 1456-1467. [In Japanese]

BU